2023 45th Annual International Conference of the IEEE Engineering in Medicine & Biology Society (EMBC) | 979-8-3503-2447-1/23/$31.00 ©2023 IEEE | DOI: 10.1109/EMBC40787.2023.10340382

A computational and experimental mechanical study of nanocomposites for 3D printed scaffolds with a new geometry

S.V. Kallivokas*, L. Kontaxis, I. Kakkos,
D. Deligianni, V. Kostopoulos, G. K. Matsopoulos, *Member, IEEE*

***Abstract*— We present a combined study of the mechanical properties of 3D printed scaffolds made by nanocomposite materials based on polycaprolactone (PCL). The geometry and dimensions of the three different systems is the same. The porosity is 50% for all systems. Distributions of von-Mises strains and stresses, and total deformations were obtained through Finite Element Analysis (FEA) for a maximum amount of force applied, in a compressive numerical experiment. Also compressive experiments were performed for both raw and 3D nanoconposite scaffolds.**

I. Introduction

Bio-composite scaffolds provide temporary mechanical support for bond and tissue regeneration. In this direction, additive manufacturing and especially 3D bioprinting has significantly boosted the research and development in bond and tissue regeneration in recent years [1]. In order to propose a new candidate with excellent geometry for the scaffolds, it is important to study the microstructure of the porous scaffolds as they play a vital role in bone and tissue regeneration [2]. Several researchers in the recent years are focusing on 3D printed scaffolds from biopolymers as a matrix material studying the mechanical, structural and other properties [3]–[7]. Deng et al. [4] studied the titanium-based composites with a porosity of 65% and a number of different geometries. Akesh et al. used Finite Element Analysis (FEA) and Representative Volume Elements (RVE) method to study the maximum stress distributions and mechanical properties of boron nitride nanotubes (BNNTs)-reinforced gelatin (G) and alginate (A) hydrogel [6]. Olivares et al. used also FEA method to study the mechanical and fluid properties in gyroid and hexagonal scaffolds of 55% and 70% porosity [5]. Also effort has been done using as a bulk or either a matrix polycaprolactone (PCL) [8], [9] as PCL is a proper candidate for tissue regeneration, due to its' high mechanical properties [10]. Recently, it has been found that it has a good match with the heart's electrical conductivity [9]. Here we propose a new candidate for scaffold materials, with a rectangular geometry that has been manufactured from a 3D printer based on PCL and composites of this as a matrix, due to the high biocompatibility that PCL has [9], [10] and the selected fillers. We carried out structural and mechanical characterization in both computational and experimental ways, in PCL and it's composites on the given geometry.

*Corresponding author
This work is supported by the BIOBON3D project under the Operational Program "Competitiveness, Entrepreneurship and Innovation (EPAnEK)", ESPA 2014-2020, and Intervention II "Business Partnerships with Research Organizations" of the Joint Action of State Aid and is co-financed by Greece and the European Union (MIS-5129423).
S. V. Kallivokas, I. Kakkos and G. K. Matsopoulos are with the Biomedical Engineering Laboratory, school of Electrical and Computer Engineering, National Technical University of Athens, Greece, Zografou 157 73, Greece

L. Kontaxis, V. Kostopoulos and D. Deligianni are with the Mechanical Engineering Department, University of Patras, Greece, University Campus 26504, Rio Achaia

II. Methods

A. Computational work

In order to take a more detailed image for the micro level of porous scaffolds we used the Finite Element Analysis (FEA) method to analyze the structure of the system. For the given rectangular geometry, as we present in the figure 1, and for the same dimensions, 5x5x5 mm^3, with 50% porosity, we applied a range of instant forces, with a maximum force up to 500 N in order to compress the systems normally. We applied the force each time in the opposite direction of the *y* axis and we kept fixed the *xz* level, in the bottom layer of the scaffold. To obtain accurate results, a mesh "sensitivity analysis" was performed in a representative case for a compressive load, from low forces up to 500N using a face size 0.05–0.2 mm. The analysis was based on the deviation between the mesh size and the produced results regarding the average and maximum results of the distributions of total deformation, von-Mises (equivalent) strains and von-Mises (equivalent) stresses. After this evaluation we chose a mesh size of 0.1 mm with a mesh element quality >75%, as a result of a deviation between different meshes and the structural results. The mesh size with <1.3% difference in the sensitivity analysis was used in the final simulations. The size of the mesh outside the scaffold region was decreased gradually from 0.2 mm to 0.05 mm. Once the mesh was created, the three-dimensional meshing process was common for all cases. We started the discretization using an element face size of 0.2 mm with 169498 elements and a mesh element quality of >63%, and reached a mesh element size of 0.05 mm with 911393 elements with a mesh metric quality ~83%. In all cases the element type is tetrahedral.

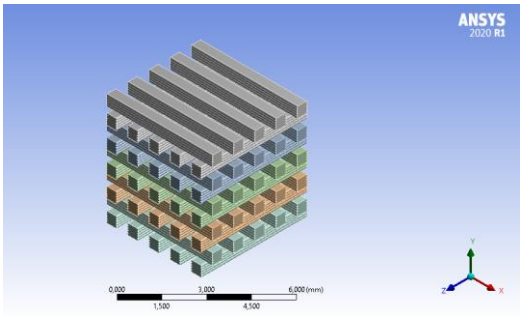

Figure 1. 3D printed scaffold's geometry with dimensions 5x5x5 mm^3.

This work is licensed under a Creative Commons Attribution 3.0 License.
For more information, see http://creativecommons.org/licenses/by/3.0/

In figure 1 above we see the scaffold's geometry with cubic dimensions of 5x5x5 mm^3. The process of design from CAD package was supplemental layer by layer, mimicking the additive manufacturing process. Each layer crosses the previews one, having 90 degrees cross-section along the *y*-axis.

B Experimental work

Oxidized multiwall carbon nanotubes (MWCNTs), with an outside diameter of 48-78 nm and with purity greater than 96% were purchased from Nanografi Nanotechnology (Ankara, Turkey), while chitosan (CS) of low and medium molecular weight was purchased from Glentham (Corsham, U.K.). The PCL of an 80.000 avg molecular weight was purchased from Thermo Scientific (Waltham, Massachusetts, USA). The MWCNTs were functionalized with the low and medium molecular weight chitosan. The MWCNTs reached 40% weight fraction regarding the low molecular weight chitosan (250.000 avg) and were denoted as L40/100 (PCL_LNG), while in the case of medium molecular weight chitosan (1.250.000 avg) the MWCNTs weight fraction was 35%, and thus denoted as M35/100 (PCL_MNG). The two different functionalized MWCNTs were added to a PCL matrix at a 5% weight fraction. Compression tests were carried out according to ASTM D0695 by means of a conventional testing machine (Monsanto Tensometer 20, St. Louis, Missouri, USA), at room temperature, for both pure and reinforced PCL. In the next step we printed in a 3D printer all specimens with dimensions 5x5x20 mm^3, for raw materials and 5x5x5 mm^3 for scaffolds while in all cases a constant crosshead speed of 10 mm/min was applied. Subsequently, 3D printed scaffolds were manufactured in a rectangular geometry as seen in Fig. 1 and were tested under compression at a constant crosshead speed of 10 mm/min, as well. The scaffolds were 3d-printed with the model 3DISON AEP by ROKIT (Seoul, South Korea).

III. CALCULATIONS AND RESULTS

A. Computational Work

In table 1 we present the mechanical and structural results of total deformation and von-Mises strains and stresses of the three scaffolds in the given geometry. We inserted as an input in the library of ANSYS package the compressive moduli that were measured in the laboratory, in raw materials of PCL, PCL_LNG, ad PCL_MNG, the temperature of experiment and the Poisson ratios from the literature [11]. Subsequently, we applied a number of forces, from 100 N up to 500 N performing a compressive numerically tests, in the opposite direction of *y* axis. Afterwards, we calculated the mean average of the distributions of both total and average total deformation, and the von-Mises stresses and strains. In table 1 we present the results. Also we present images of the system during the compressive numerically test, imprinting the maximum deformation, and the maximum von-Mises strains and stresses. We are able to see that the stresses and strains are concentrated in the cross-area regions of the system, during the normal compression (see fig.2). The same behavior quantitatively is happening in the whole range of forces, and in the rest scaffolds, PCL_LNG and PCL_MNG.

On the other hand, as we see in the figure 3, the total deformation distribution, has higher deformed areas are on the higher layer, due to the normal force that is applied direct to this layer, and decreasing from layer to layer, as the cross areas, absorb the stress.

Table I. Distributions of maximum and average total deformation, equivalent Strains and Stresses values for PCL and PCL composites for the maximum load of 500N.

System	***Total def. Max (mm)***	***Total def. Avr. (mm)***	***Eq. Elastic Strain Max.***	***Eq. Elastic Strain Avr.***	***Eq. Stress Max. (MPa)***	***Eq. Stress Aver. (MPa)***
PCL	1.86	0.85	1.11	0.22	205.2	43.8
PCL_ LNG	1.30	0.60	0.80	0.15	207.5	43.3
PCL_ MNG	1.01	0.46	0.61	0.12	207.4	43.3

In table 1, we see that in terms of total deformation (both maximum and average) and equivalent strains (also both maximum and average) PCL_LNG has the highest values between the composites. A reason for this is due to the higher molecular weight of filler in PCL_LNG, in contrast with the smaller one in PCL_MNG. PCL bulk has higher values of strains and total deformation, between all of them. In terms of stresses, we do not see major differences, and this makes us assume that the MWCNT's and the CS do not play significant role in this direction, giving just a slight increase of the equivalent stresses in the composites.

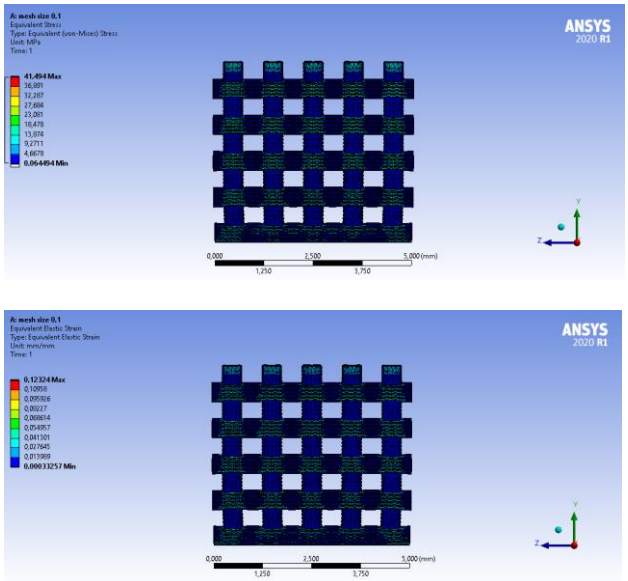

Figure 2. Profiles of equivalent stresses and strains, in the *y* axis, after a load of an instant force 100 N, for PCL scaffold.

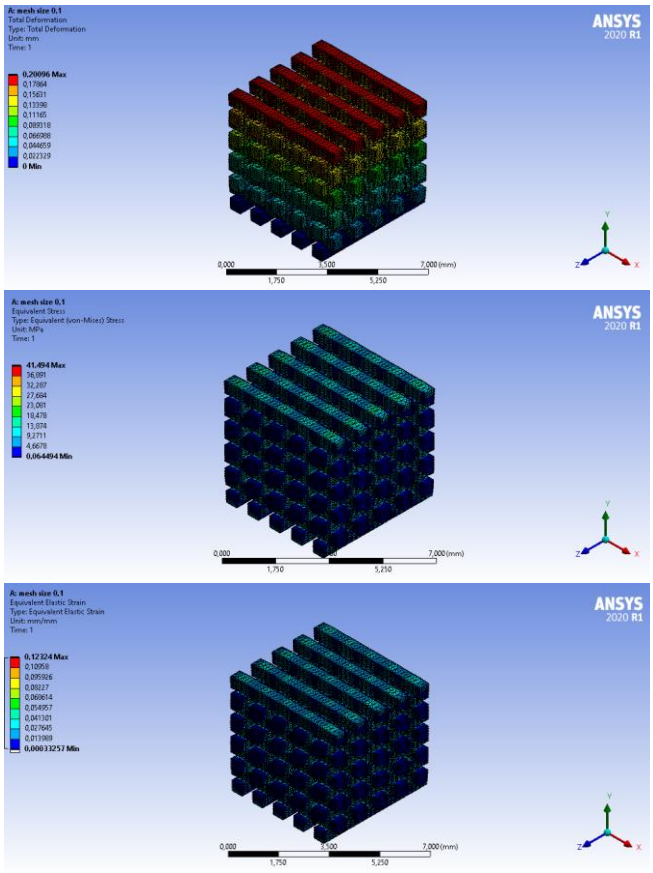

Figure 3. Total deformation, equivalent stress and strain for the PCL scaffold for an instant force of 100N

B. *Experimental work*

Compressive experiments performed in the laboratory for raw materials. The specimens were tested under compression at a constant rate of 10 mm/min. The results are presented in Tables II and III. We see that the PCL_MNG in terms of raw material has a higher compressive modulus that almost doubles that of pure PCL. Also, the PCL_LNG has a higher compressive modulus than the pure PCL. This is attributed to the reinforcement introduced, which restricts the molecular chains' movement, thus increasing the compression modulus. Finally, the PCL reinforced with the medium molecular weight chitosan (PCL_MNG) provides better reinforcement than the low molecular one (PCL_LNG), since longer polymer chains indicate greater entanglement of the polymer chains, resulting in a higher compressive modulus. From the other hand, in the 3D printed scaffolds, (see table III).

Table II. Experimental values for compressive moduli for raw materials.

Materials	***Compression Modulus (MPa)***
PCL	0.237
PCL_LNG	0.34
PCL MNG	0.441

Table III Experimental values for compressive moduli and ultimate strengths for 3D printed polymer scaffolds.

Materials	***Compressive Modulus (MPa)***	***Ultimate Strength (MPa)***
PCL	62.3	14.6
PCL_LNG	116	12.7
PCL MNG	109	16

In a similar fashion, compression moduli of the reinforced 3D printed scaffolds are higher of the PCL compressive modulus. However, in this case, the compression moduli of the reinforced specimens were nearly identical, indeed within experimental error margins. What was observed during the experiments was that PCL_LNG was more brittle compared to the PCL_MNG, which correlates to the fact that PCL_LNG has shorter chitosan chains.

IV. CONCLUSION

We see a trend between the experimental compressive modulus and the computational distributions of equivalent stress and strain, and total deformation of the PCL_LNG, making it, into a proper candidate for the scaffolds for our cubistic geometry. Taking into account the total deformation and the equivalent strains, we can say that PCL bulk also is a good candidate for scaffolds, having also higher ultimate strength. Although, a more detailed research must be given in the direction of mechanical characterization in both experimental and computational way for these systems in our geometry.

ACKNOWLEDGMENT

We would like to thank also Professor C. M. Athanassopoulos and Dr. A. Tsirogianni for the preparation of polymers, from the Chemistry Department University of Patras. Also, we thank Professor Lampeas, from the Laboratory of Technology & Strength of Materials (LTSM), from the department of Mechanical Engineering & Aeronautics University of Patras, for ANSYS software.

REFERENCES

[1] S. M. Giannitelli, D. Accoto, M. Trombetta, and A. Rainer, "Current trends in the design of scaffolds for computer-aided tissue engineering," *Acta Biomater.*, vol. 10, no. 2, pp. 580–594, 2014, doi: 10.1016/j.actbio.2013.10.024.

[2] P. Ouyang *et al.*, "Hydromechanical mechanism behind the effect of pore size of porous titanium scaffolds on osteoblast response and bone ingrowth," *Mater. Des.*, vol. 183, p. 108151, 2019, doi: 10.1016/j.matdes.2019.108151.

[3] R. Dwivedi *et al.*, *Polycaprolactone as biomaterial for bone scaffolds: Review of literature*, vol. 10, no. 1. Craniofacial Research Foundation, 2020.

[4] F. Deng, L. Liu, Z. Li, and J. Liu, "3D printed

Ti6Al4V bone scaffolds with different pore structure effects on bone ingrowth," *J. Biol. Eng.*, vol. 15, no. 1, pp. 1–13, 2021, doi: 10.1186/s13036-021-00255-8.

[5] A. L. Olivares, È. Marsal, J. A. Planell, and D. Lacroix, "Finite element study of scaffold architecture design and culture conditions for tissue engineering," *Biomaterials*, vol. 30, no. 30, pp. 6142–6149, 2009, doi: 10.1016/j.biomaterials.2009.07.041.

[6] A. B. Kakarla, I. Kong, S. G. Nukala, and W. Kong, "Mechanical Behaviour Evaluation of Porous Scaffold for Tissue-Engineering Applications Using Finite Element Analysis," *J. Compos. Sci.*, vol. 6, no. 2, pp. 1–10, 2022, doi: 10.3390/jcs6020046.

[7] M. Suffo and C. J. López-Marín, "A comparative study of turbulence methods applied to the design of a 3d-printed scaffold and the selection of the appropriate numerical scheme to simulate the scaffold for tissue engineering," *Appl. Sci.*, vol. 12, no. 1, 2022, doi: 10.3390/app12010191.

[8] A. Zieliński and B. Majkowska-Marzec, "Whether Carbon Nanotubes Are Capable, Promising, and Safe for Their Application in Nervous System Regeneration. Some Critical Remarks and Research Strategies," *Coatings*, vol. 12, no. 11, p. 1643, 2022, doi: 10.3390/coatings12111643.

[9] S. Pok, F. Vitale, S. L. Eichmann, O. M. Benavides, M. Pasquali, and J. G. Jacot, "Biocompatible carbon nanotube-chitosan scaffold matching the electrical conductivity of the heart," *ACS Nano*, vol. 8, no. 10, pp. 9822–9832, 2014, doi: 10.1021/nn503693h.

[10] M. A. Woodruff and D. W. Hutmacher, "The return of a forgotten polymer - Polycaprolactone in the 21st century," *Prog. Polym. Sci.*, vol. 35, no. 10, pp. 1217–1256, 2010, doi: 10.1016/j.progpolymsci.2010.04.002.

[11] F. Rezgui, M. Swistek, J. M. Hiver, C. G'Sell, and T. Sadoun, "Deformation and damage upon stretching of degradable polymers (PLA and PCL)," *Polymer*, vol. 46, no. 18, pp. 7370–7385, 2005, doi: 10.1016/j.polymer.2005.03.116.